BIBECHANA
Vol. 22, No. 2, August 2025, 171-180

ISSN 2091-0762 (Print), 2382-5340 (Online)
Journal homepage: http://nepjol.info/index.php/BIBECHANA
Publisher:Dept. of Phys., Mahendra Morang A. M. Campus (Tribhuvan University)Biratnagar

A spectroscopic study of the merging dwarf galaxy PGC 007782

Shankar Timalsina, Daya Nidhi Chhatkuli*

[1]*Department of Physics, Tri-Chandra Multiple Campus, Tribhuvan University, Ghantaghar, Kathmandu, Nepal*
*Corresponding authors. Email: chhatkulidn@gmail.com

Abstract

We conducted a detailed spectroscopic study of PGC 007782, an interacting emission-type dwarf galaxy. This study utilized optical spectra of emission lines to explore the system of interacting dwarf galaxies. Gaussian fitting techniques were used to examine the main spectral lines (H_α, H_β, H_γ, SII, OIII, and NII) and determined their Gaussian parameters. Our investigation mainly focused on nine prominent emission lines with wavelengths ranging from 4342 Å to 6733 Å. Among which, H_α is the most prominent line with a peak intensity of 72.16 $\times$ 10^{-17} erg/s/cm^2/Å corresponds to the central wavelength of 6564 Å. With the flux of 2.93 $\times$ 10^{-17} erg/s/cm^2/Å, the NII line is the weakest at the central wavelength of 6550 Å. The SII line has the highest FWHM value of 4.04 Å, indicating a higher gas temperature. Each of these emission lines exhibits a nearly perfect Gaussian profile, with a coefficient of determination exceeding 92%. Utilizing the H_α line, the star formation rate of PGC 007782 is calculated to be 0.014 $M_\odot$ yr^{-1}, indicating that active star formation is concentrated at the galaxy's core. The calculated value of Balmer decrement is 4.02 which is higher than the normal value indicating the light coming out from this galaxy is being blocked by the dust particles. With oxygen abundance of 8.31dex, the physical and morphological characteristics of PGC 007782 confirmed this galaxy as a metal-poor, actively star forming blue compact dwarf (BCD) galaxy.

Keywords
Dwarf Galaxy, Galaxy merger, Balmer decrement, Star formation rate

Article information
Manuscript received: December 13, 2024; Revised: January 8, 2025; Accepted: May 20, 2025
DOI https://doi.org/10.3126/bibechana.v22i2.72618

1 Introduction

Galaxies frequently come together and merge to form bigger and complex ones. This process (hierarchical) of structure formation, happens frequently in regions of many galaxies, like clusters or groups. According to Smith et al. (2018) [1], galaxies interact and collide frequently in this crowded region. When galaxies merge, gas clouds are compressed causing new stars to form quickly leading to a burst of star formation [2]. Merging galaxies also create long streams of gas and stars known as tidal,

pulled out by gravity. These tails come together and change the shape of the galaxy [3].

Dwarf Galaxies are small but significant for study as they can trigger starbursts-short periods of intense star formation. Galaxy formation can be affected by these starbursts, particularly in nearby galaxies [4]. These bursts of stars are very helpful for understanding how galaxies change over time and give information about dark matter [5].

When a small galaxy merges with bigger ones, the merging process mixes the gas inside the galaxies spreading heavy elements (metals) throughout the galaxy. However, the amount of metal (metallicity) can be temporarily decreased when two galaxies of similar size merge [6].

Scientists use spectra of dwarf galaxies to know about them. Dwarf galaxies contain stars of different gas and chemical compositions as studied by Lee et al. (2018) and Smith et al. (2020) [7, 8]. H_α and OIII emission lines can reveal areas where stars are still forming [9,10]. Information about how the galaxy's stars and metals have changed over time can be provided by absorption features [11,12]. These studies show a wide range of histories of dwarf galaxies.

As star formation rate (SFR) measures how quickly gas and dust in the galaxy turn into stars, SFR is essential for understanding how galaxies grow and evolve. Star formation rate of the universe has changed significantly over time. It reached its peak around redshifts z$\sim$ 2. This period of intense star formation is called cosmic noon [13]. The star formation rate reached its maximum at that time due to the dense gas contained in the galaxies. About 75% of all stars in the universe formed between the redshift of z$\sim$2.5 to z$\sim$0. The SFR steadily declined after this peak. Studying these periods provides valuable insight into galaxy evolution.

Many factors affect SFR. Under the effect of gravity, higher gas density and pressure cause gas to collapse, leading to faster star formation [14]. When the metallicity is high, that is, if the amount of elements heavier than Hydrogen and Helium is high, higher metallicity cools the gas better, making it easier to form stars [15]. Barnes & Hernquist in 1996 [16] studied the SFR in galaxies. According to them, when galaxies merge, tidal forces squeeze gas clouds, causing bursts of star formation. Magnetic fields have positive as well as negative influences on SFR. Magnetic fields either slow down by holding gas clouds together or gathering gas to those places where stars can form easily [17]. Another factor that affects the SFR is Active Galactic Nuclei (AGN). AGN affects the SFR by either pushing gas to form stars or heating and removing gas, stopping star formation [18, 19].

To study galaxy evolution of the universe, understanding SFR is crucial. A very high SFR can finish the gas reservoir of the galaxy, stopping future formation of stars and changing the galaxy's shape and types of stars [20]. Elements like Iron and carbon are released when Supernova explodes, mixing these elements with surrounding gas and dust, enriching these materials in the galaxy. Next generation of stars and even planets use this enriched gas and dust [21]. Studying SFR overtime provides valuable information about the forces that shape them, helping us to know how galaxies and the universe have changed [22].

In this project, we present the spectroscopic study of a low redshift (z = 0.0180), metal-poor, antenna type actively star-forming merging Blue Compact Dwarf (BCD) galaxy PGC 007782 and calculate its SFR and oxygen abundance.

2 Sample Selection

Due to their small size, low surface brightness, and dimness, dwarf galaxies are challenging to detect since they are hard to separate from surrounding stars and background noise. While massive galaxy interactions have been extensively studied, there's a lack of research on interactions between low-mass dwarf galaxies. For this reason, studying dwarf galaxies is crucial. Scientists can also learn much about dark matter—an unknown substance that makes up a large fraction of the universe. Not only that, because of their more easily studied stellar populations, these areas provide important information on the formation and evolution of stars.

Dwarf galaxies, the building component of larger galaxies, provides information about the origin and evolution of galaxies as well as how they interact with one another and with larger galaxies. To delve deep into, we have selected a low redshift (z = 0.0180) merging dwarf galaxy PGC 007782 from a catalog by Paudel et al., (2018) [23] located at R. A. (J2000): 02 h 02 m 38.7600 s, Dec.(J2000): -09 d 22 m 13.080 s.

Morphologically, PGC 007782 is an antenna type galaxy 77.06 Mpc far from us. Its (g – r) color is 0.30 mag and has no satellite. The apparent g and r band AB magnitude of the galaxy are 15.43 mag and 15.13 mag respectively. The radial velocity of the galaxy taken from NED is 5396 km/s. Only one neighbor is found within the search criteria (within a sky-projected distance of less than 700 kpc, and a relative line-of-sight radial velocity of less than $\pm$700 km/s). The SDSS DR 12 optical image of the galaxy PGC 007782 and its spectrum are shown in **Fig. 1 (a)** and **1 (b)** respectively. We can see that the galaxy is elongated along the N-S direction and has an antenna in the southern region. The antenna indicates that it is an interacting galaxy. In the optical wavelength range of 3500 Å to 7500 Å, there

are many emission lines which are due to different elements like Hydrogen, Helium, Oxygen, Nitrogen, Sulphur and so on. The spectrum shows that the galaxy is an emission type.

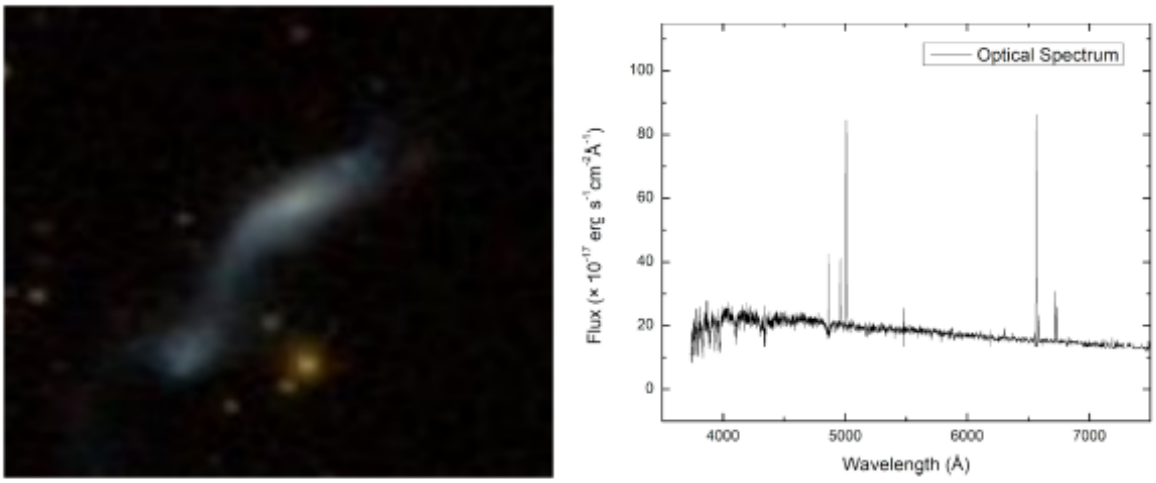

Figure 1: (a) The SDSS DR 12 optical image of interacting galaxy PGC 007782. (b) The optical spectrum of the galaxy PGC 007782.

3 Data Analysis

To study the star-forming properties of the merging dwarf galaxy PGC 007782, this galaxy has been selected as a sample. The study will utilize data from the Sloan Digital Sky Survey (SDSS), obtaining its spectrum and analyzing it using Origin software. The galaxy spectrum will be extracted by using Aladin software. Aladin software provides a flexible viewer for astronomical images. With it, users can interactively analyze and explore astronomical objects and their attributes by seeing multi-wavelength photos and superimposing catalogs. Aladin 2.5 is used to extract the archival data of the dwarf galaxy PGC 007782 from its FITS file. The data will be used to plot the optical spectrum by using Origin software of version 8. Origin software is widely used in the field of astronomy and is one of the simplest method to create high-quality graphs, performs statistical analysis, and supports curve fitting and automation and analyze graphs. A Gaussian fitting technique will be used to model data that follows a Gaussian distribution or simply normal distribution. It involves fitting a Gaussian function to a dataset to calculate parameters as mean, standard deviation, which characterizes the central tendency and spread of the data respectively. This model is also applied to curve fitting, signal processing and experimental analysis in a variety of fields. We measure the physical parameters of each emission line by Gaussian fits, including total flux, Full Width Half Maximum (FWHM) and best-fit coefficient. Mathematically, Gaussian distribution function is given as;

$$F_G(x) = \frac{1}{\sqrt{2\pi\sigma^2}}\, e^{\frac{-(x-\mu)}{2\sigma^2}^2}$$

Where, x represents a normal random variable, μ represents mean deviation and, σ represents the standard deviation of the distribution. FWHM is the width at which maximum amplitude drops to half a width. A width referred to as the full width half maximum (FWHM) is reached at this point. We choose nine emission lines and their Gaussian parameters based on the greater intensity, which will be described in this work along with their Gaussian parameters. We will calculate the hydrogen line ratio and the star formation rate (SFR). Kennicutti's [24,25] empirical formula is used for calculating the SFR providing a reliable, empirical methods to calculate the star formation rate based on observed H_α luminosity. Mathematically, Kennicutt's empirical formula is given by equation (1).

$$\text{SFR } (M\odot \text{year}^{-1}) = 7.9 \times 10^{-42}\ \Sigma\ L\ (H_\alpha)\ (\text{ergs s}^{-1}) \quad (1)$$

where $L(H_\alpha)$ represents the total luminosity of H_α line which will be calculated by using Gaussian fits. $L(H_\alpha)$ = Area of Gaussian fit $\times\ 10^{-17} \times 4R^2$ (ergs s^{-1}). R is the radius of the sphere which is calculated as: $R = D \times 3.08 \times 10^{24}$ cm. Here, D is the luminosity distance of the galaxy in Mpc. The gas phase metallicity will be calculated by using the empirical formula given in equation (2) provided by Marino et. al. (2013) [26].

$$12 + \log(O/H) = 8.743 + 0.462 \times \log\ (NII/H_\alpha) \quad (2)$$

4 Results and Discussion

Gaussian fitting curves of the main emission lines, i.e., H_α, H_β, H_γ, SII, OIII and NII of the dwarf galaxy PGC 007782 are obtained. Among these, SII, OIII and NII are in duplet. H_α, H_β, H_γ, are the Balmer lines. Only the prominent emission lines H_α, H_β, $OIII_{5008}$ and NII_{6585} are shown in **Fig. 2**. Observed data are presented by the black dots and the red solid line represents the Gaussian fit for the observed data. It shows that the observed data follows the Gaussian distribution more accurately.

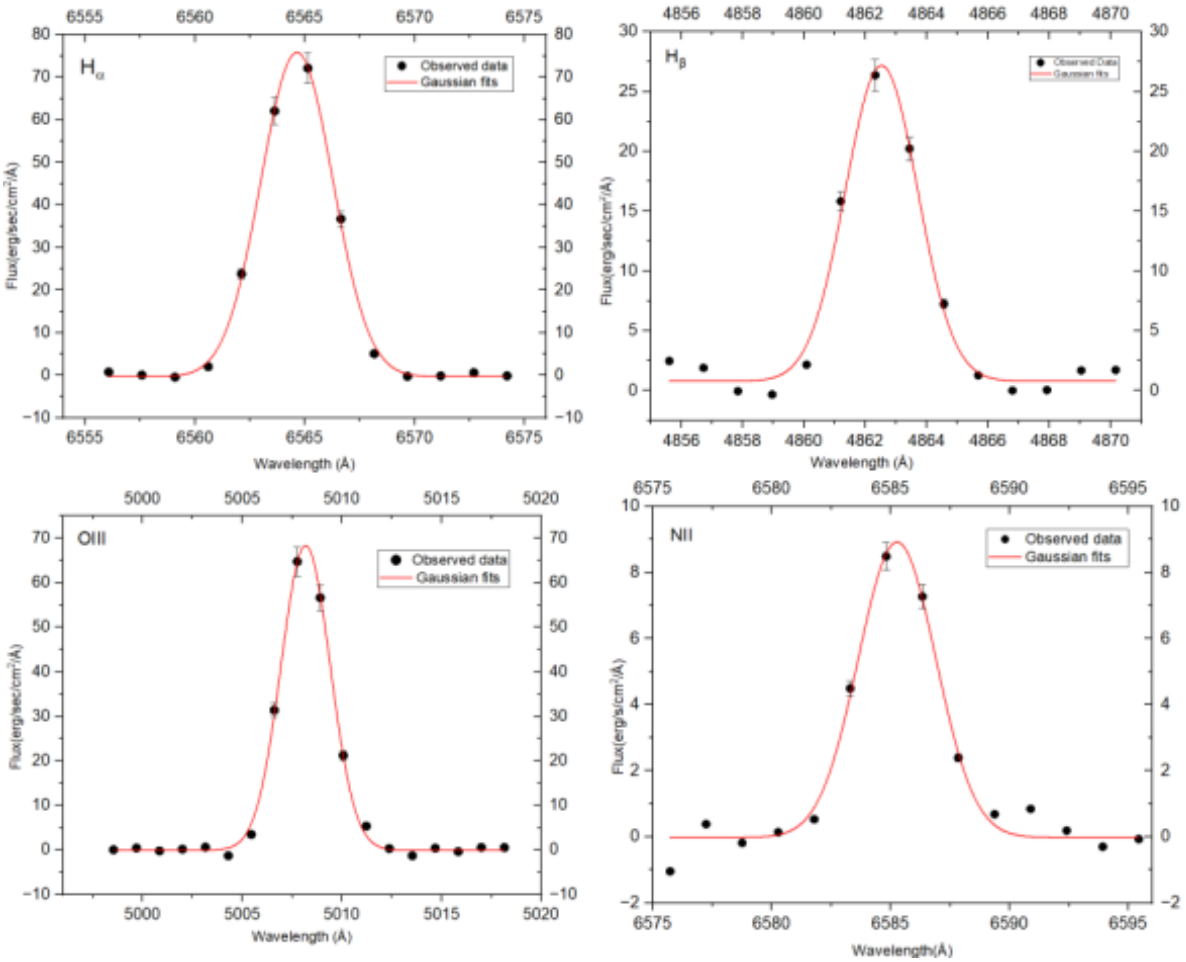

Figure 2: The Gaussian fitting curves of four prominent emission lines H_α, H_β OIII and NII are shown.

Gaussian parametric values of the dwarf galaxy PGC 007782 obtained after fitting of Gaussian curves are presented in **Table 1**. The names of the chosen emission lines are shown in the first column whereas, column two and three show the wavelength corresponding to peak intensity (λ_p) in Å and the peak intensity λ_p in ($\times 10^{-17}$ erg/s/cm^2/Å) respectively. The fourth, fifth, sixth, seventh and eighth columns represent FWHM in Å, area of Gaussian curve in ($\times 10^{-17}$ erg/s/cm^2/Å), height of Gaussian curve in ($\times 10^{-17}$ erg/s/cm^2/Å), off set and coefficient of determination value respectively.

Table 1: Gaussian parameters of the observed emission lines of dwarf galaxy PGC 007782.

Elements	λ_p (Å)	I_p	FWHM (Å)	Area	Height	Offset	R-square
Hγ	4342	26.23	2.49	68.18	25.72	+0.0036	0.97
Hβ	4863	26.35	2.77	77.75	26.37	-0.0043	0.98
[O III]	4960	19.97	2.79	65.12	21.95	+0.0042	0.99
[O III]	5008	64.74	2.91	211.73	68.38	+0.0004	0.99
[N II]	6550	2.93	3.65	10.79	2.78	+0.0004	0.92
Hα	6564	72.16	3.85	312.60	76.20	+0.0025	1.00
[N II]	6585	8.48	3.84	36.54	8.94	-0.0049	0.98
[S II]	6718	15.70	4.04	50.78	11.80	-0.0013	0.99
[S II]	6733	10.74	3.85	66.75	16.30	-0.0046	1.00

Through a careful investigation of the emission lines, significant new information about the physical property and underlining process has been obtained. H_α emission lines come out with highest peak intensity of 72.16 $\times$ 10^{-17} erg/s/cm^2/Å, corresponding to the wavelength of 6564 Å suggesting active star formation within the galaxy. This prominent line implies that necessary hydrogen gas is being ionized by young hot stars.

Similarly, second and third peak intensity of 64.74 $\times$ 10^{-17} erg/s/cm^2/Å and 26.35 $\times$ 10^{-17} erg/s/cm^2/Å respectively for lines OIII and H_β lines at 5008 Å and 4863 Å, shows high-excitation regime that are probably driven by energetic processes near hot star or an active galactic nucleus (AGN). Balmer series lines H_γ and HH_β show nearly comparable peak intensity. These lines give important information on the temperature and density of the ionized gas, as well as the constant ionization state throughout the galaxy [27]. NII lines are the weakest emission lines, indicating a reduced excitation or amount of nitrogen in the ionized part of the galaxy with a peak intensity of 8.48 $\times$ 10^{-17} erg/s/cm^2/Å and 2.93 $\times$ 10^{-17} erg/s/cm^2/Å, corresponding to the wavelength 6785 Å and 6750 Å respectively.

The SII curve shows the greatest value of FWHM that is 4.04 Å, indicating that the SII line has the widest width at half of its maximum intensity, compared to the other lines in the above table. Also, a larger FWHM means the spectral line is wider which indicates that a larger range of wavelengths are being occupied by the line's emissions process or transition. This happens for a number of reasons such as increased temperature, increased turbulence, or a wider velocity dispersion of the substance that is emitting or absorbing [28, 29]. A large FWHM value, sometimes indicates a wider spread of velocity within the emitting or absorbing gas or a more complicated physical environment.

The table also provides measurement of the FWHM for various other spectral lines observed in optical spectra, like the Balmer line H_γ has the lowest FWHM of 2.49 Å, indicating its width when its intensity is at half of its peak. This smaller FWHM indicates that the spectral line is narrower. This narrower line indicates that the substance, that is emitting or absorbing, is limited to a narrower range of temperature or velocity. This can happen in those environments where the motion or temperature of the gas is more ordered or where there is less turbulence.

The greatest Gaussian area corresponds to the H_α emission lines, which is 312.60 $\times$ 10^{-17} erg/s/cm^2/Å. A larger area denotes a stronger or more intense emission or absorption feature, since it suggests a greater total energy emitted or absorbed over the whole width of the spectral line. In contrast, NII has the smallest area that is 10.79 $\times$ 10^{-17} erg/s/cm^2 /Å, suggesting a lower total energy flux or intensities, showing weaker or less intense spectral features. OIII has the largest offset of 0.0042 representing a greater discrepancy between the major data point and the expected value from the models or the theoretical prediction. Similarly, NII has also the smallest offset of -0.0049, indicating there is least discrepancy between the measured data point and the expected values.

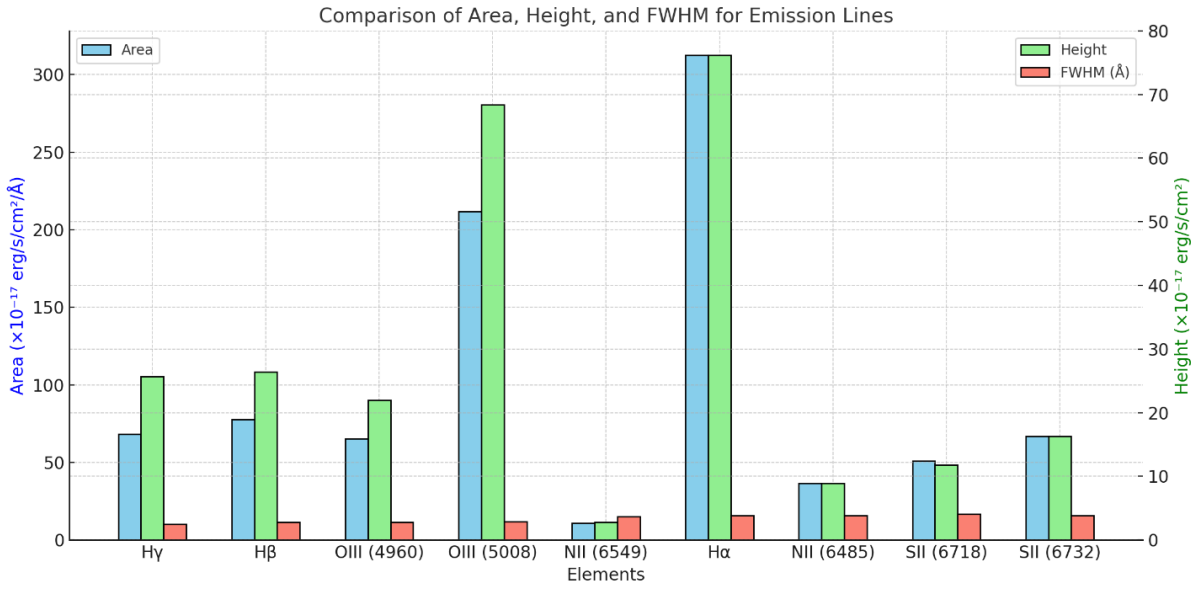

Figure 3: Comparison of the physical parameters such as area, height and FWHM for emission lines. Different colors represent different parameters. Green color represents height of the emission lines, sky blue color indicates area of the fitting curve and red color represents the FWHM value, for their respective emission lines.

Graph plot **Fig. 3** compares three Gaussian parameters such as area, height and FWHM values of the emission lines. These features indicate total energy emitted by the lines (flux), velocity dispersion or broadening of the gas (turbulence) and, peak intensity of the line. Emission lines with larger areas usually have peak intensity [30]. For example, H_α line has the largest area and highest peak intensity. Above plot also shows a broad FWHM value can still have a high area. However, their peak heights are lower due to the distribution of energy over a wider wavelength range. For example, SII lines have moderate area but SII lines' broader FWHM reduces their peak heights compared to lines like OIII (5008), which has a narrow width [31]. Similarly, emission lines having narrower width might still have higher peak height. The OIII (5008) line has a small value of FWHM but still has a high peak, maybe due to this line emitting gas which is less turbulent or moving uniformly.

A combination of high area, peak height, and broad FWHM suggests intense star formation accompanied by significant gas turbulence. Modest area, modest height of the peak and narrow FWHM indicates less active regions with lower gas densities velocities. Lastly, low area, low height of the peak and broad FWHM indicates low density gas with significant turbulence or outflow.

Through the careful examination of emission lines of dwarf galaxy PGC 007782, significant details on the physical parameters and star-forming activity are revealed. The line ratio of H_α to H, is calculated to be 4.2. This is the significant deviation from the expected value of 2.8. This variation indicates the possibility of internal dust reddening within the galaxy, as dust dims the light from both lines differently, making the H_α line a comparatively greater appearance. Dust-rich environments within the galaxy might have affected the observed features of the emission lines as suggested by the high H_α to H_β line ratio [32].

The star formation rate for dwarf galaxy PGC 007782 after extinction correction is determined to be 0.0136 M year^1 by using equation (1). This calculated value indicates that the galaxy is actively producing stars at the faster rate, but as compared to the larger more massive galaxies, this galaxy forms new stars at a slower pace. The calculated value of SFR also indicates that this galaxy's current star formation is well after the cosmic noon and is still forming stars at a lower rate in the local universe. In contrast, as galaxies have consumed much of their gas and external fueling mechanism are less frequent, the local universe (z∼0) shows the steady decline in SFR. This rate for PGC 007782 while which is not as high as some other star forming galaxies nevertheless, indicates a strong star forming activity particularly for a dwarf galaxy.

The emission line metallicity is calculated to be 8.31, using the line ratio of NII and H_α emission lines in equation (2). It shows that PGC 007782 is a metal-poor galaxy, indicating that this is a young or not fully evolved dwarf galaxy, which is typically a blue compact dwarf galaxy. These BCDs, small, irregular galaxies with rapid star formation rates appear blue, due to the presence of a larger

number of young hot stars [33]. The metal poor state of PGC007782 indicates that it has not experienced significant chemical enrichment, a characteristic common to star-forming galaxies that has not yet accumulated a major heavy element accumulation. The calculated parameters of the galaxy are summarized in the **Fig. 3.**

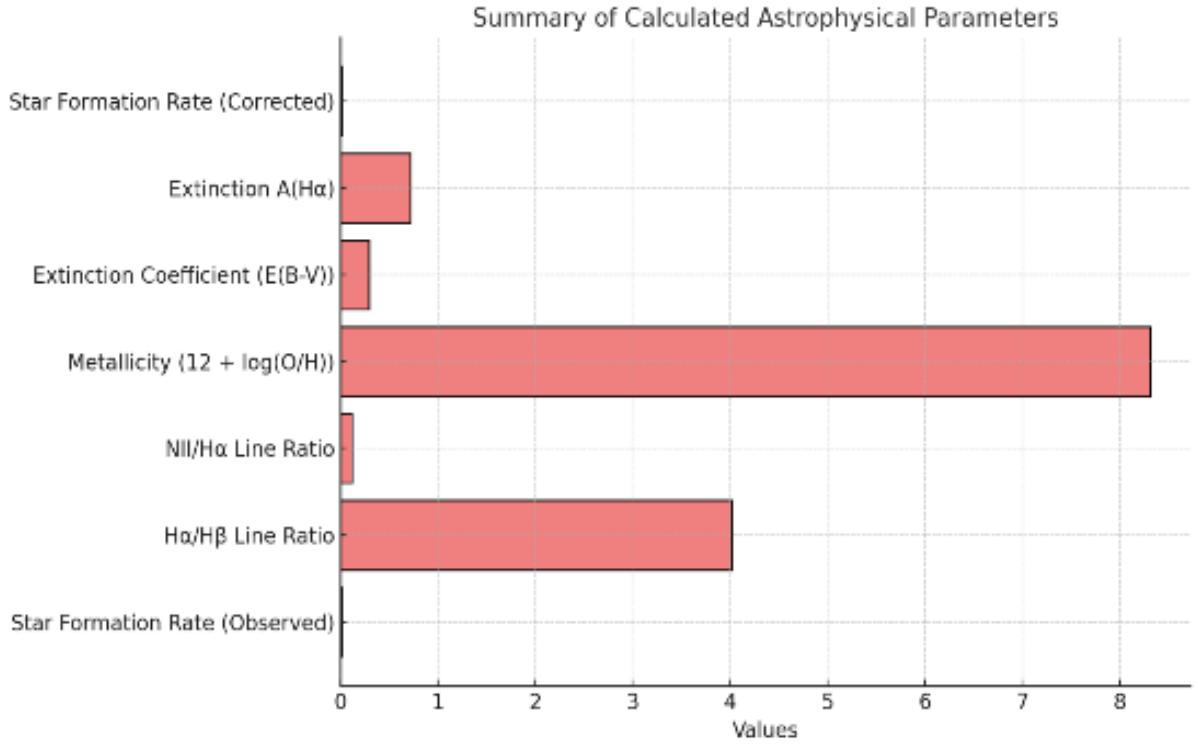

Figure 4: Figure showing the horizontal bar graph summarizing the calculated parameters.

Initially, by measuring the area under the Gaussian fitting for the H_α line, the calculated value for SFR is 0.0084 $M_M\odot yr^1$. The light emitted from these galaxies has to pass through dust, which blocks some of the light, especially at shorter wavelengths. The Balmer decrement i.e., the ratio of H_α and H_β, indicates the presence of dust. The theoretical value for Balmer decrement is 2.28, but what we calculate is 4.02, which is significantly higher. The high ratio of H_α to H_β indicates that much of the H_β line is blocked by the dust, whereas H_α line is not affected by the dust, making it stronger and indicating high star formation rate [34]. The extinction coefficient was applied to the H_α flux and calculated to be 0.291, indicating dust along the line of sight to the observed object. This calculated value shows a moderate amount of dust between the observer and the object. After accounting for extinction, which reflects the true star formation activity, the calculated SFR is $0.014 M_M\odot$ yr^{-1}, which means dust hides some of the star formation activity. We use the line of [NII] and H_α to calculate the metallicity i.e., the abundance of elements heavier than hydrogen and helium, which is calculated to be 8.31 dex. This value suggests that PGC 007782 has fewer heavy elements, indicating that this galaxy is a young or not fully evolved.

5 Comparison with Other Works

The SFR obtained from spectroscopic study for SDSSJ222726.64+120539.8 and SDSSJ162753.47+482529.3 is 0.010 $M_M\odot$ yr^{-1} and 0.016 $M_M\odot$ yr^{-1} respectively [35], which is similar to the SFR of PGC 007782 showing that all have moderate star formation activity. Metallicity of these galaxies are nearly the same showing all these Galaxies are metal poor. The SFR of CG 0315 is calculated to be 0.051 $M_M\odot$ yr^{-1} [36], which is higher than the SFR of PGC 007782, indicating star forming activities are happening more in CG 0315. With an effective radius of 4.5 arcsecond and half-light radius of 2.60 arcsecond, CG 0315 is declared to be BCD similar to PGC 007782.

The SFR for NGC 5194 (M51a) is calculated to be 3.4 $M_M\odot$ yr^{-1} [37]. This shows that NGC 5194 (M51a) forms stars at the rate of around 261 times the star formation rate of PGC 007782, indicating rapid star formation process. SFR using the H_α line method calculated for SDSS J134326.99+431118.7

is 0.019 $M_{M}\odot$ yr^{-1} [38] which is slightly higher than that of PGC 007782 and has a more active star forming environment. This was also conducted by using the optical spectrum of the major emission lines.

SFR of galaxy UGC 4483 is calculated to be 0.008 $M_{M}\odot yr^{-1}$ [39]. This value of 0.008 $M_{M}\odot^{-1}$ is slightly lower than the SFR of PGC 007782. That means, PGC 007782 forms stars approximately 1.6 times higher. This indicates that the higher SFR galaxy has more active star forming regions or possibly more efficient star formation processes. Consequently, the galaxy PGC 007782 with the higher star forming rate undergoes more rapid evolutionary changes compared to UGC 4483.

This comparison highlights that galaxies can vary significantly in how fastly the formation starts, influenced by factors like their size, type and the amount of gas available for Star formation. The higher rate observed in this galaxy suggests that it is currently undergoing more active star formation compared to the standard reference value. These measurements are important for understanding the process of star formation across different galaxies and their evolution over cosmic time.

6 Conclusion

The system of interacting dwarf galaxies is examined through optical spectra of emission lines. Strongest or major emission lines are Gaussian fitted in this project. We present the result of a thorough study of the emission lines of the dwarf galaxy PGC 007782 with great attention given to the principal spectral lines H_{α}, H_{β}, H_{γ}, SII, OIII, and NII. Gaussian fitting techniques were used to determine the FWHM, wavelength, peak intensities and other relevant parameters of these lines.

Based on the observation and calculations, the following conclusions are drawn.

(a) The H_{α} emission line is the most prominent. Similarly, the NII emission line is weakest reflecting reduced energy releases from this element.

(b) The SII line has the largest FWHM indicating that, SII line is wider than other emission lines, possibly caused by higher temperature or more movement of the gas in the galaxy.

(c) Areas were represented by total flux under the gaussian curves, with H_{α} having the largest area, indicating strong emission. Similarly, the NII line has the smallest area indicating weak emission.

(d) PGC 007782 is classified as a metal-poor actively star-farming Blue Compact Dwarf (BCD) galaxy indicated by SFR (0.0136 $M_{M}\odot yr^{-1}$) and its metallicity (8.31dex).

(e) Emission lines exhibit a nearly perfect Gaussian profile, with a regression coefficient exceeding 92 % showing gaussian fits for the lines were accurate.

Acknowledgements

This project used the archival images and spectra from the Sloan Digital Sky Survey (SDSS) (http://www:sdss.org/collaboration/credits.html). So, we are thankful to SDSS.

References

[1] A. B. Smith, V. Bromm, and A. Loeb. The dynamics of dwarf galaxy mergers. *Monthly Notices of the Royal Astronomical Society*, 475(3):3185–3196, 2018.

[2] J. E. Barnes and L. Hernquist. Formation of bulges and black holes in galaxy mergers. *The Astrophysical Journal Letters*, 370:L65, 1991.

[3] A. Toomre and J. Toomre. Galactic bridges and tails. *The Astrophysical Journal*, 178:623–666, 1972.

[4] M. G. Jones and M. Johnson. Star formation in dwarf galaxy mergers. *The Astrophysical Journal*, 871(1):78, 2019.

[5] J. C. Lee et al. The star formation history of the universe from the epoch of reionization to the present. *Nature Reviews Astronomy Astrophysics*, 8:1–14, 2020.

[6] L. Michel-Dansac et al. Gas accretion onto galaxies. *Astronomy Astrophysics*, 484(2):405–418, 2008.

[7] H. Lee et al. Stellar populations in dwarf galaxies. *Monthly Notices of the Royal Astronomical Society*, 478(2):192–205, 2018.

[8] A. B. Smith et al. Gas dynamics in dwarf galaxies. *The Astrophysical Journal*, 812(1):34–47, 2020.

[9] E. D. Skillman et al. Emission line analysis of dwarf galaxy spectra. *The Astronomical Journal*, 147(3):58–71, 2014.

[10] D. R. Weisz et al. Star formation rates in dwarf galaxies. *The Astrophysical Journal Letters*, 775(2):L29–L35, 2018.

[11] M. Geha et al. Metallicity gradients in dwarf galaxy spectra. *Monthly Notices of the Royal Astronomical Society*, 467(3):3182–3195, 2017.

[12] A. Gallazzi et al. Stellar abundances in dwarf galaxy spectra. *The Astrophysical Journal*, 634(2):1002–1014, 2005.

[13] P. Madau and M. Dickinson. Cosmic star-formation history. *Annual Review of Astronomy and Astrophysics*, 52:415–486, 2014.

[14] M. R. Krumholz, A. Dekel, and C. F. McKee. Turbulence and star formation in molecular clouds. *The Astrophysical Journal*, 754(2):71, 2012.

[15] D. K. Erb, A. E. Shapley, M. Pettini, C. C. Steidel, K. L. Adelberger, and M. E. Dickinson. The stellar mass dependence of the c iv 1549 equivalent width distribution at z 2. *The Astrophysical Journal*, 646(1):107, 2006.

[16] J. E. Barnes and L. Hernquist. Galaxy collisions in three dimensions. *The Astrophysical Journal*, 467(2):799–811, 1996.

[17] P. Padovani and D. Galli. The cosmic star formation rate from z = 2 to z = 0. *Monthly Notices of the Royal Astronomical Society*, 427(3):2057–2069, 2012.

[18] P. F. Hopkins, L. Hernquist, T. J. Cox, S. Dutta, and B. Rothberg. A unified model for the co-evolution of black holes and galaxies. *The Astrophysical Journal*, 679(1):156–187, 2008.

[19] A. C. Fabian. Observational evidence of active galactic nucleus feedback. *Annual Review of Astronomy and Astrophysics*, 50:455–489, 2012.

[20] E. W. Peng and M. D. Weinberg. The impact of globular cluster systems on galaxy evolution. *The Astrophysical Journal*, 532(1):505–521, 2000.

[21] V. Bromm and R. B. Larson. The first galaxies. *Annual Review of Astronomy and Astrophysics*, 42:79–118, 2004.

[22] A. M. Hopkins and J. F. Beacom. On the normalization of the local galaxy luminosity function. *The Astrophysical Journal*, 651(2):142–149, 2006.

[23] S. Paudel, C. Sengupta, and S. J. Yoon. Kug 0200 096: Dwarf antennae hosting a tidal dwarf galaxy. *The Astronomical Journal*, 156(4):17, 2018.

[24] C. R. Jr. Kennicutt. Star formation in galaxies along the hubble sequence. *Annual Review of Astronomy and Astrophysics*, 36:189–231, 1998.

[25] C. R. Jr. Kennicutt. Star formation in galaxies along the hubble sequence. *Annual Review of Astronomy and Astrophysics*, 36:189–231, 1998.

[26] R. A. Marino and et al. The o3n2 and n2 abundance indicators revisited: improved calibrations based on califa and te-based literature data. *Astronomy and Astrophysics*, 559, 2013.

[27] L. J. Kewley and M. A. Dopita. Using strong lines to estimate abundances in extragalactic h ii regions and starburst galaxies. *The Astrophysical Journal Supplement Series*, 142(1):35–52, 2002.

[28] L. J. Kewley, M. A. Dopita, R. S. Sutherland, and et al. Theoretical modeling of starburst galaxies. *Astrophysical Journal*, 556(1):121–140, 2001.

[29] B. M. Peterson. *An Introduction to Active Galactic Nuclei*. Cambridge University Press, 1997.

[30] Robert C. Jr. Kennicutt. Star formation in galaxies along the hubble sequence. *Annual Review of Astronomy and Astrophysics*, 36(1):189–232, 1998.

[31] C. M. Gaskell. Direct evidence for gravitational domination of the motion of gas within one light-week of the central object in ngc 4151 and the determination of the mass of the probable black hole. *Astrophysical Journal*, 287:509–514, 1984.

[32] D. Calzetti. Dust and star formation in galaxies: A historical perspective. *Publications of the Astronomical Society of the Pacific*, 113(783):1449–1465, 2001.

[33] Y. I. Izotov and T. X. Thuan. The nature of blue compact dwarf galaxies. *The Astrophysical Journal*, 511(2):639–659, 1999.

[34] S. P. Gautam, A. Silwal, N. Lamichhane, A. K. Jha, and B. Aryal. Study of star formation rate and metallicity of the low redshift ($z < 0.02$) dwarf galaxies. *BIBECHANA*, 18(2):43–49, 2021.

[35] D. N. Chhatkuli, S. Paudel, A. Sedhain, and B. Aryal. Structural parameter of a merging compact dwarf galaxy cg 0315. *Journal of Institute of Science and Technology*, 27(2):85–89, 2022.

[36] D. N. Chhatkuli, S. Paudel, and B. Aryal. A detailed morphological and spectroscopic study of merging dwarf galaxy pgc 030133. *Journal of Nepal Physical Society*, 7(4):28–35, 2021.

[37] D. Calzetti, R. C. Jr. Kennicutt, L. Bianchi, D. A. Thilker, D. A. Dale, C. W. Engelbracht, and D. Lindler. Star formation in ngc 5194 (m51a): The panchromatic view from galex to spitzer. *The Astrophysical Journal*, 633(2):871–893, 2005.

[38] D. N. Chhatkuli, S. Paudel, and B. Aryal. A detailed morphological and spectroscopic study of merging dwarf galaxy pgc 030133. *Journal of Nepal Physical Society*, 7(4):28–35, 2021.

[39] J. Brinchmann, S. Charlot, S. D. M. White, and C. A. Tremonti. The physical properties of star-forming galaxies in the low-redshift universe. *Monthly Notices of the Royal Astronomical Society*, 351(4):1151–1179, 2004.